A Nature Portfolio journal



https://doi.org/10.1038/s43247-025-02895-w

U-Pb calcite age dating of fossil eggshell as an accurate deep time geochronometer



Ryan T. Tucker ^{1,2} ⊠, Kira E. Venter¹, Cristiano Lana¹,³, Eric M. Roberts⁴, Tsogtbaatar Chinzorig²,⁵,6, Khishigjav Tsogtbaatar⁵ & Lindsay E. Zanno ^{1,2,6,7,8,9}

Earth's sedimentary rock record is the primary archive for biotic, environmental, and climatic trends in deep time. Reconstructing these patterns requires a high-resolution geochronologic framework. This remains a significant challenge for many terrestrial ecosystems and an acute problem for some of the world's most important Mesozoic and Cenozoic fossil records. Overcoming this issue requires frontier approaches, such as directly dating fossils, long considered untenable. Here, we test the reliability of novel LA-ICP-MS U-Pb calcite dating and elemental mapping of non-avian dinosaur eggshells to produce accurate "burial ages." We directly dated fossilized dinosaur eggs recovered from the Western Interior Basin of North America, producing ages within 5% of high-precision ages from bracketing ash beds. We then directly dated dinosaur eggs from Upper Cretaceous strata within Mongolia's famous yet poorly age-constrained Gobi Basin, providing the first radioisotopic age for these deposits. Geochemical data coupled with trace elemental mapping indicate early uptake of uranium (U) in non-avian dinosaur eggshells via sediment contact, consistent with findings from Quaternary avian eggs. Calcified eggs, having evolved over 250 million years ago, offers a promising experimental methodology for determining the age of globally distributed fossil assemblages and recovering temporal, environmental, and ecological data from a single fossil.

Studying evolutionary and ecological processes in deep time requires refined geological age estimates for paleontological data. Unfortunately, confident temporal frameworks are difficult to achieve for many of the world's most important fossil assemblages^{1,2}. Currently, the gold standard for dating continental sedimentary deposits is U-Pb or Ar-Ar dating of interbedded volcanic deposits (e.g., ash beds, lava flows)³⁻¹⁰. However, the presence of datable volcanic units is typically restricted to sedimentary basins proximal to volcanic arc systems in convergent margins, meaning that alternative dating methods are required for many continental interior basins^{10,11}. In addition, many methods available for resolving the age of marine strata (e.g., biostratigraphy; Sr-isotope stratigraphy) are unavailable or less precise for dating terrestrial deposits.

Recent investigations on alternative geochronometers in terrestrial systems have focused on studies that date biological materials and various carbonate minerals within sedimentary rocks. The direct dating of fossilized bone and teeth has met with variable success 12-16. These studies highlight

ongoing issues associated with dating biological materials, which may act as open systems affected by fossilization, diagenetic alteration, and overprinting^{17–24}. On the other hand, carbonate U-Pb geochronology has been increasingly applied to a broader range of geologic materials (e.g., calcite veins, lacustrine limestones, soil carbonates, and speleothems) with continued improvements in methods, standards, and applications^{12,21,22,24}; however, application of the methods as a direct-dating method for fossil taxa is in its infancy. The unique ultra- and microstructure of biocalcite found in eggshells permits nuanced diagenetic screening before dating. This, coupled with the fact that calcified-egg-laying vertebrates have been a diverse component of Earth's terrestrial ecosystems since the Paleozoic, underscores the potential of fossil eggshell as a novel geochronometer in deep time^{25–34} (Fig. 1).

Although U-series dating has been tested and applied to dating Quaternary eggshells^{25–27}, in situ laser ablation U-Pb calcite age dating of fossil eggshells has yet to be tested in deep time. If validated, this approach could

¹Department of Earth Sciences, Stellenbosch University, Private Bag X1 Matieland, Stellenbosch, South Africa. ²Paleontology, North Carolina Museum of Natural Sciences, 121 W. Jones St., Raleigh, NC, USA. ³Department of Geologia, Universidade Federal de Ouro Preto, Ouro Preto (MG), Brazil. ⁴Department of Geology and Geological Engineering, Colorado School of Mines, Golden, CO, USA. ⁵Institute of Paleontology, Mongolian Academy of Sciences, Ulaanbaatar, Mongolia. ⁶Department of Biological Sciences, Campus Box 7566, NC State University, Raleigh, NC, USA. ⁷Department of Geology, Field Museum of Natural History, Chicago, IL, USA. ⁸Natural History Museum of Utah, University of Utah, 301 Wakara Way, Salt Lake City, UT, USA. ⁹Vertebrate Paleontology, Oklahoma Museum of Natural History, Norman, OK, USA. Ee-mail: tucker@sun.ac.za

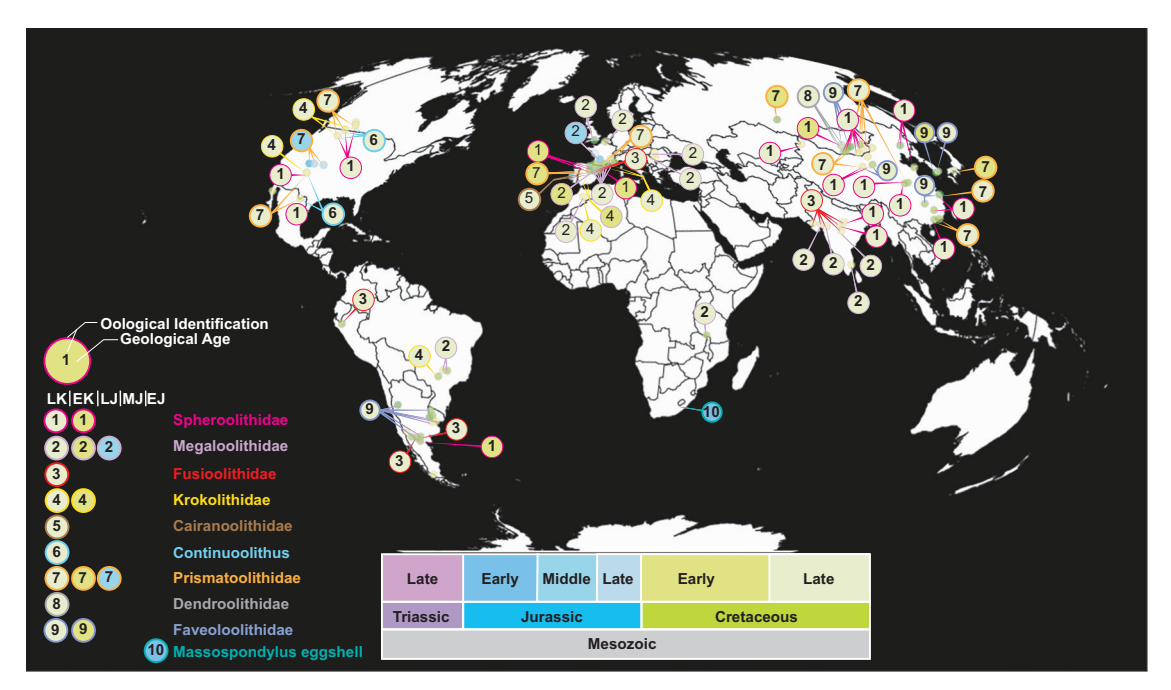


Fig. 1 | Global distribution map of fossilized egg discoveries (spanning the Mesozoic-Cenozoic), highlighting the abundance of fossilized eggs and eggshells across space and time in continental sedimentary successions (Figure references 55,59,60). Map and fossil egg localities complied using the PBDB (CC0 International License; https://paleobiodb.org/#/).

greatly expand the range of continental sedimentary successions amenable to radioisotopic dating. Here, we present results from the first in-situ U-Pb calcite dating and trace elemental mapping of non-avian dinosaur eggshells via Thermo Neptune multi-collector inductively coupled plasma mass spectrometer (LA-MC-ICP-MS) from two different Cretaceous fossil localities. The first set of specimens originates from the Mussentuchit Member of the Cedar Mountain Formation in the Western Interior Basin (USA), which is bracketed by precisely dated ash beds⁷, serving as a control group. The second set represents newly discovered egg clutches (2022) from the Teel Ulaan Chaltsai locality, in the Eastern Gobi Basin of Mongolia. Lacking datable volcanics, the age of the beds at Teel Ulaan Chaltsai remains uncertain, with conflicting Early vs. Late Cretaceous age assignments by different workers^{35–37}, making this an ideal test case for using eggshell dating to resolve this stratigraphic issue (Fig. 2). Therefore, our study investigates this approach and offers a unique, broadly applicable alternative for dating continental, vertebrate-bearing deposits worldwide.

Methods

In situ U-Pb calcite age dating results of eggshells from Utah and the Gobi locality (Fig. 2) were acquired using an LA-MC-ICP-MS coupled to a Photon Machines 193 nm laser ablation (LA) system at the Universidade Federal de Ouro Preto, following an adapted method³⁸. Samples were ablated in a helium atmosphere and mixed with argon and nitrogen, with the MC-ICP-MS optimized for sensitivity while minimizing oxide formation and fractionation. Laser parameters included 110 µm spot sizes, 5 Hz repetition, and 6 J cm $^{-2}$ fluence, yielding a penetration depth of <10 μ m for NIST SRM-614. U-Pb and Pb-Pb ratios were normalized^{22,39,40}, calibrated using WC-1 and NIST SRM-614, applying mass bias and interelement fractionation corrections. Data reduction was conducted via SATURN software, and results were reported at a 2σ confidence interval. Tera-Wasserburg plots were used for regression, and uranium concentrations were estimated against WC-1. Age uncertainties included both analytical and external standard errors. See Supplementary Data 1 and 2 for detailed results.

Trace element data were acquired at the Department of Earth Sciences, Stellenbosch University, using a Thermo Scientific Element 2 sector field ICP-MS coupled to a Resolution 193 nm excimer laser ablation system. Analyses were conducted in low mass resolution mode, and the following

isotopes were measured: Mg²⁴, Si²⁹, Ca⁴⁴, Ti⁴⁹, Mn⁵⁵, Fe⁵⁶, Cu⁶⁵, Zn⁶⁶, Sr⁸⁸ Y⁸⁹, Zr⁹⁰, Ba¹³⁷, La¹³⁹, Ce¹⁴⁰, Pr¹⁴¹, Nd¹⁴⁶, Sm¹⁴⁷, Eu¹⁵³, Gd¹⁵⁷, Tb¹⁵⁹, Dy¹⁶³, Ho¹⁶⁵, Er¹⁶⁶, Tm¹⁶⁹, Yb¹⁷², Lu¹⁷⁵, Pb²⁰⁸, Th²³², and U²³⁸. Data processing and quantitative imaging were performed using Saturn TE Map, a custom Python-based software developed for high-resolution LA-ICP-MS elemental mapping. The software reconstructs the 2D spatial layout of line scan data using laser stage logs and applies pixel-wise quantification based on certified reference materials. Raw intensity data were background-corrected using a global average derived from background segments of standard files only and normalized using External Calibration with Internal Standardization (ECIS). NIST SRM-612 was used as the primary calibration standard, and NIST SRM-614 and BHVO-2 were employed as secondary quality control materials to monitor accuracy and precision. Resulting elemental concentrations (in ppm) were visualized as individual heatmaps and RGB composites. Region-of-interest (ROI) tools were used to extract per-element statistics (mean, standard error, min, max), supporting interpretation of trace element zoning and U/Pb distributions within eggshell ultra- and microtextures.

Results Geochronology

Three eggshell pieces were selected from a partial clutch of theropod dinosaur eggs (NCSM 33576-324 A)^{7,41-43}, excavated from the "Deep Eddy" locality (Fig. 2a), referable to eggshell ootype Macroelongatoolithus carlylei⁴³ and laid by oviraptorosaurian dinosaurs (Theropoda). Selected samples were approximately 1.8 mm in thickness, lacking any internal or external diagenetic or recrystallization features; however, minor taphonomic weathering of the ultra- and microstructure in the form of fractures and fissures was identified. Initial screening for uranium (U) concentration identified the most promising regions of the eggshells for dating, with elevated U concentrations, specifically the mammillae lining the internal surface and the high-relief ornamental nodes along the external surface of the eggshell, characteristic of elongatoolithid eggs (Fig. 3A). The surfaces between the external ornamental knobs contained either high concentrations of common Pb (Pbc) or too little U for analysis. Two independent rounds of U-Pb LA-MC-ICP-MS analysis were performed on seven eggshells (Round 1: 96 spot analyses on four eggshell pieces; and Round 2: 176 spot analyses). For both runs, most spots exhibited U concentrations

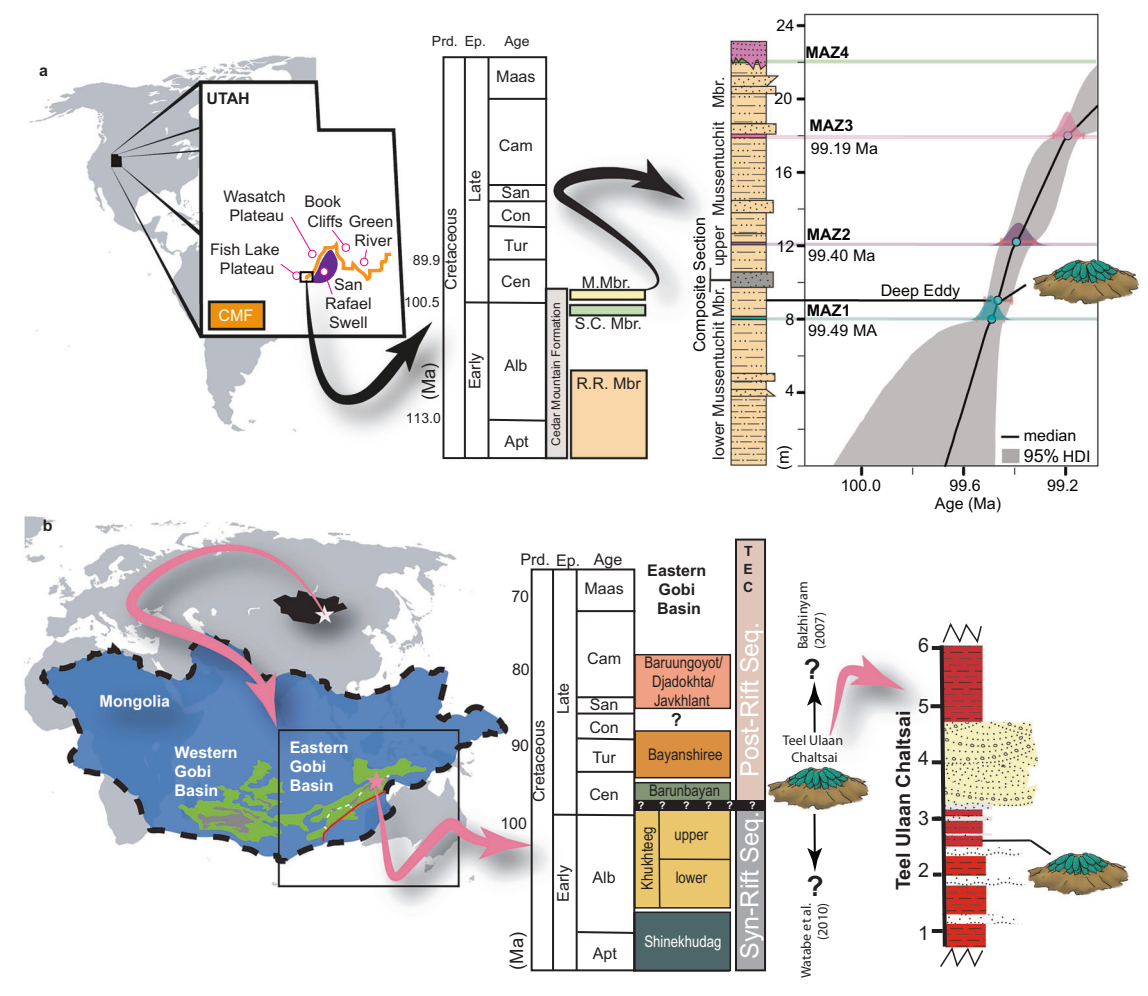


Fig. 2 | **Location of sample sites. a** Mussentuchit Member, Cedar Mountain Formation, Central Utah (USA) with high-precision CA-ID-TIMS U-Pb zircon geochronology and age model for formation shown relative to the location of eggs sampled in this study at the "Deep Eddy" site⁶¹; and **b** The Teel Ulaan Chaltsai nest horizon eggshell sample sites, Sainshand Sub-basin of the Eastern Gobi Basin (Images modified from^{7,42,55,60}). Note that the age of this extensive nest horizon and

eggshell horizon (~3.5 km long) has alternatively been interpreted as either belonging to the Lower Cretaceous syn-rift stratigraphy vs. the Upper Cretaceous post-rift stratigraphy (Figure references/A1,42,61-67). Global Maps modified from "Wikimedia Commons" CC BY-SA 4.0 (https://commons.wikimedia.org/wiki/File:BlankMap-World-with-Circles_17_April_2024.svg).

ranging from 0.012 to 3.5 ppm, with an average of 0.3 ppm (Supplementary Data 1). Of the total 272 spot analyses, 34 contained no detectable U and did not yield meaningful U-Pb ratios. The remaining spots align remarkably well along a regression line with an upper intercept of 0.829 (207 Pb/ 206 Pb) and a lower intercept age of 94.7 \pm 1.3/2.3 Ma (2 σ , MSWD = 1.5, n = 238). Based on the 238 single spot analyses on eggshells from sample NCSM 33576, an age of 94.7 \pm 1.3/2.3 Ma is interpreted (Fig. 3A).

Fossil eggshells (Dinosauria indet.) were collected in 2022 from four lithostratigraphically similar locations along a single, extensive horizon (3.5 km laterally, 2.5 m vertically) of dinosaur nests and isolated eggshells (interpreted as a nesting area) by a joint NCSM/SU/IP-MAS expedition (MADEx) to the Eastern Gobi Basin at Teel Ulaan Chaltsai (Mogoin Daatsyn Khuduk)³⁵⁻³⁷ (Figs. 2b, 3B). Selected samples were approximately 2.7 mm in thickness, lacking any internal or external diagenetic alteration or recrystallization, and no visible taphonomic weathering or structural deformation. Two independent rounds of U-Pb LA-MC-ICP-MS were performed on the external surface and along an internal transect through the eggshell profiles across eight individual fossil eggshells collected in situ from four different stratigraphically similar localities, MPC-D 100/1067, 100/1068, 100/1069, and 100/1070 at Teel Ulaan Chaltsai (Supplementary Data 2). The first round of dating included 120 spot analyses on eggshells from MPC-D 100/1070, 95 spot analyses on eggshells from MPC-D 100/ 1068, 72 spot analyses on eggshells from MPC-D 100/1069, and 94 spot

analyses on eggshells from MPC-D 100/1067. The second round of dating involved 48 repeat spot analyses on eggshells from MPC-D 100/1070 only. Remarkably, only four total spot analyses from both laser sessions were discarded due to very low U concentrations. Individual runs yielded consistent ages of ca. 75-77 Ma on the Tera-Wasserburg plots, including: MPC-D 100/1070 at 75.8 ± 2.0 Ma $(2\sigma, MSWD=1.8);$ MPC-D 100/1068 at 75.6 ± 2.7 Ma $(2\sigma, MSWD=0.7);$ MPC-D 100/1069 at 77.1 ± 4.0 Ma $(2\sigma, MSWD=1.4)$ and MPC-D 100/1067 at 76.6 ± 1.4 Ma $(2\sigma, MSWD=0.31)$. There is a remarkable consistency of ages (2% of the age and overlap of uncertainties) from this extensive, lithostratigraphically correlated nest horizon, providing strong support for the accuracy of the age. Combining all the ablation spot results from all four sampling sites at the Teel Ulaan Chaltsai nest horizon onto a single Tera-Wasserburg plot produces an age of $75.35 \pm 0.74/1.5$ Ma $(2\sigma, MSWD=1.4, Pbi=0.840)$ (Fig. 3B), which we interpret as the best age of this site.

Trace element mapping

Trace element mapping of the dated eggshells from both sampled localities reveals a consistent pattern of well-preserved horizontal layering in Sr, U, and Y, reflecting original biomineralisation structures and indicating excellent preservation of original eggshell ultrastructure. Sr concentrations (up to 120ppm) exhibit sharp, laterally continuous bands that align precisely with optical growth lines, indicating minimal elemental redistribution and

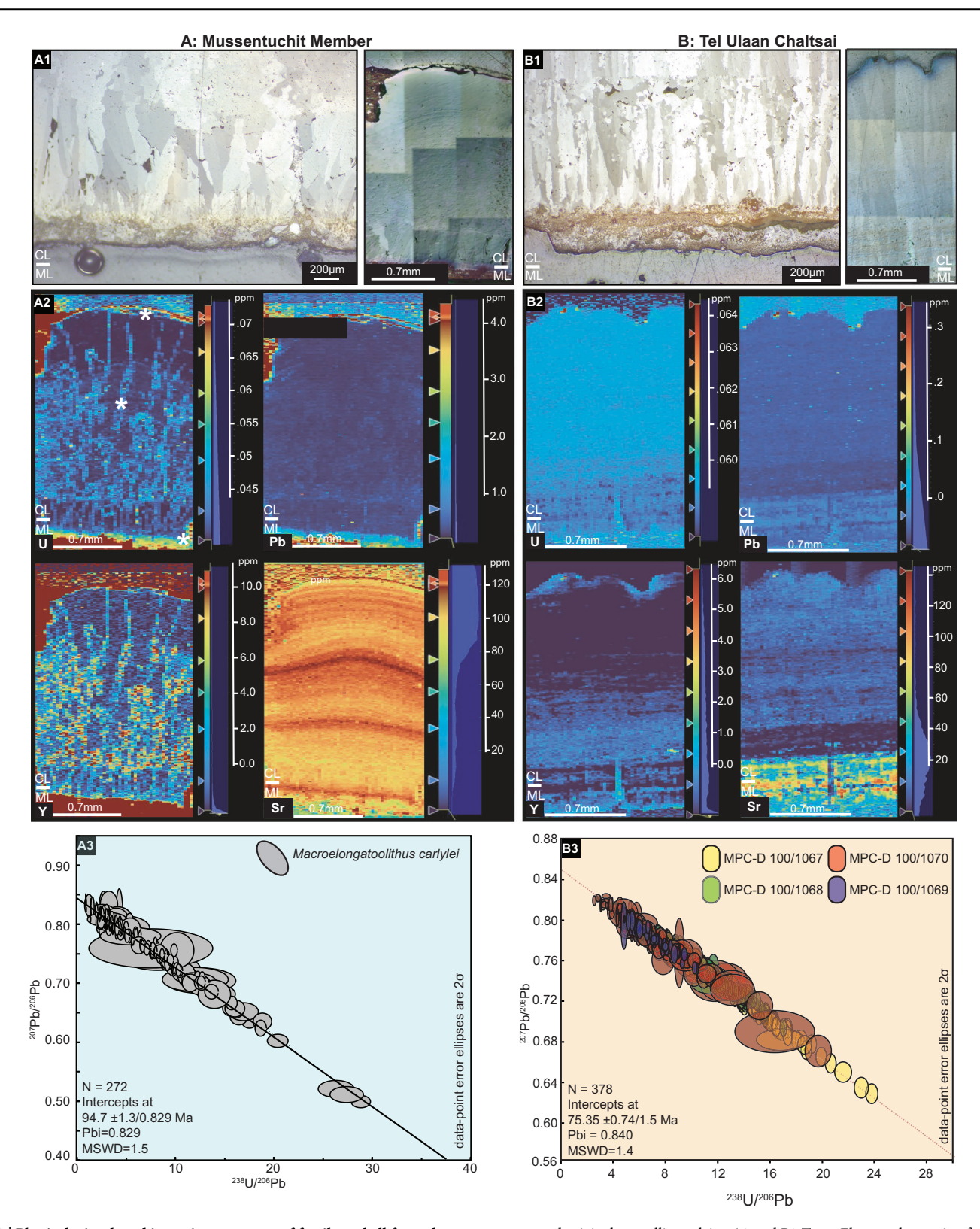


Fig. 3 | Physical, visual, and isotopic assessment of fossil eggshell from the Mussentuchit Member of the Cedar Mountain Formation and from Teel Ulaan Chaltsai in the Eastern Gobi Basin. Column A1-3, Deep Eddy site, Mussentuchit Member, Cedar Mountain Formation; B1-3, Teel Ulaan Chaltsai nest site, Eastern Gobi Basin, with A1 and B1 SEM and optical imagery, with samples exhibiting well-

preserved original crystalline calcite; A2 and B2 Trace Elemental mapping for isotopes U, Pb, Y, Sr Blagh; and A3 and B3 present U-Pb LA-MC-ICP-MS eggshell geochronology results (272 ablation spots for the Deep Eddy and 373 ablation spots for the Teel Ulaan Chaltsai nest site).

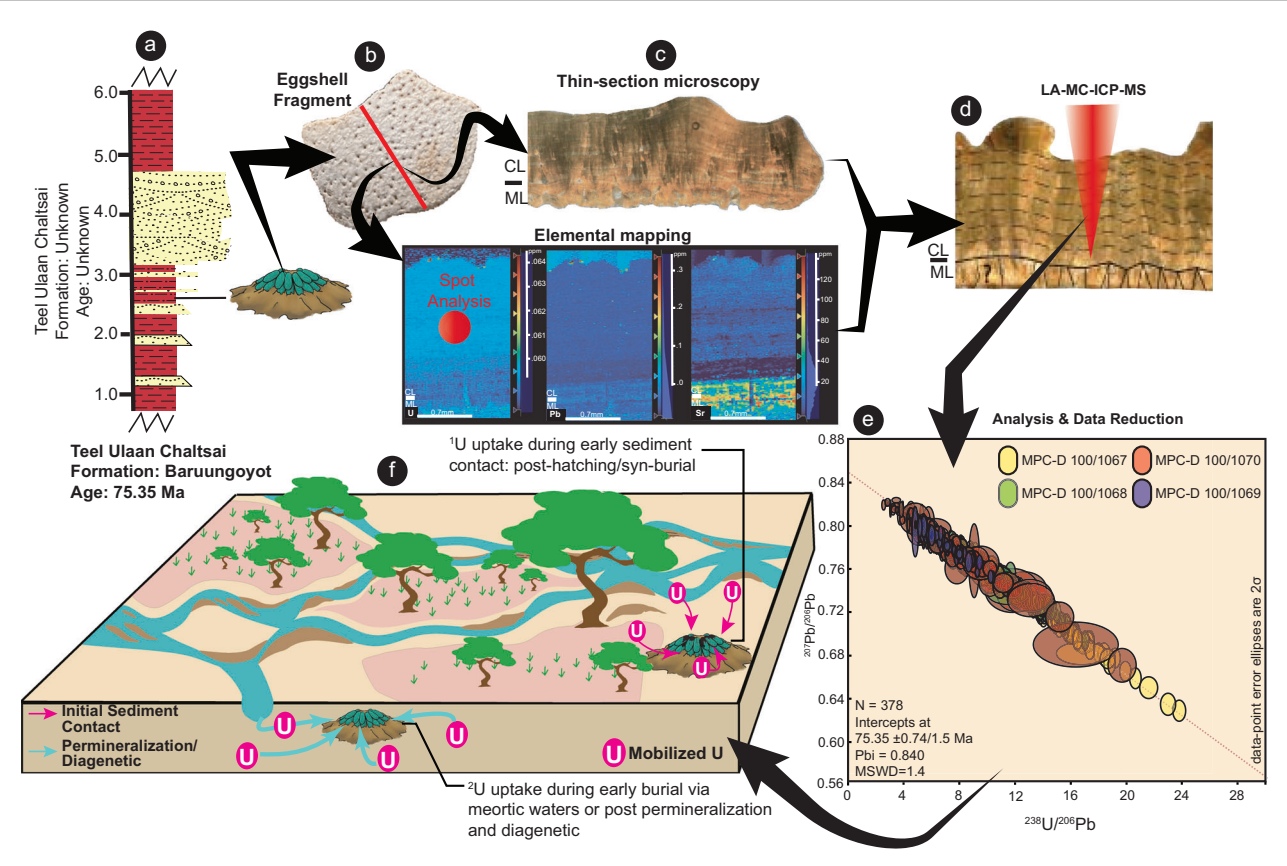


Fig. 4 | Diagram depicting the methodological pathways for in-situ U-Pb calcite dating of the eggshell and current interpretation for the uptake of original U during the early phases of sediment contact within the Mongolian-based eggshells. a Teel Ulaan Chaltsai with unknown lithostratigraphic position or age. b Collected and cleaned eggshell sample. c Eggshell histology coupled with

geochemical screening and elemental mapping. **d** Biocalcite is dated via in-situ U-Pb LA-MC-ICP-MS methods. **e** Age is calculated to help interpret the site's stratigraphy. **f** Interpretation based on data collected indicated a near syndepositional age of 75.35 Ma and lithostratigraphically coeval with the Baruungoyot Formation. Artwork via M.B. Daughty and J. Hedge.

strong preservation of primary shell chemistry in all samples. U (0.045-0.75ppm) and Y (0-10ppm) also broadly follow this layered structure in all samples; however, key differences highlight varying degrees of post-depositional alteration. MPC-D 100/1067 eggshell displays subtle vertical diffusion in U and Y, likely caused by minor fluid infiltration during early diagenesis. Whereas the NCSM 33576-324 A exhibits more prominent vertical enrichment along microfractures and porous domains, suggesting stronger and possibly prolonged exposure to sediment-derived fluids. These vertical pathways likely exploited the original pore structure of the eggshell, as well as diagenetic microfractures within the eggshell's ultrastructure, which are more pronounced in the Mussentuchit Member samples. Such features appear to have served as conduits for the migration of trace elements, which had a more significant impact on the specimens from the Mussentuchit Member. Pb remains low and spatially uniform in both specimens, supporting the interpretation that it was either immobile or introduced in negligible quantities during the diagenesis process.

Discussion

To investigate the potential for dating fossilized dinosaur eggshells via U-Pb calcite geochronology as a meaningful new chronometer in terrestrial depositional settings, we compared our Utah eggshell dating results with published U-Pb tuff and detrital zircon ages from deposits entombing NCSM 33576, a clutch of dinosaur eggs at "Deep Eddy" locality. LA-ICP-MS U-Pb detrital zircon analysis of sediments entombing NCSM 33576 yielded a maximum depositional age (MDA) of 94.5 \pm 0.9 (N = 3 at 15% filter, MSWD = 0.82) 41 ; however, a more conservative MDA based on the youngest six grains (instead of 3) yields an age of 97.1 \pm 0.83 Ma (N = 6 at 5% filter, MSWD = 1.2), which is preferred here, based on the likelihood of Pbloss in some of the youngest zircons (Fig. 3A; See Supplementary Data 3).

The conservative detrital zircon MDA of 97.1 \pm 0.83 Ma is within ~3% of the calcite U-Pb eggshell age and overlaps within the propagated uncertainty. However, a comparison of the eggshell ages with two high-precision CA-ID-TIMS U-Pb zircon ages of volcanic tuff beds overlying and underlying NCSM 33576 demonstrates that the depositional age of the nest site is slightly older than the U-Pb calcite age from the eggshell. Specifically, the underlying ash bed (MAZ1; 50 cm below) age is 99.490 + 0.057/-0.050, and the overlying ash bed (MAZ2; 70 cm above) age is 99.401 + 0.085/-0.066 (Fig. 3A)⁷ (See Supplementary Data 4). Hence, the LA-MC-ICP-MS U-Pb calcite age of $94.7 \pm 1.3/2.3$ Ma on eggshells from the Mussentuchit nest site (NCSM 33576) is roughly 4.9% younger [((99.5-94.7)/(99.5 + 99.7/ 2))*100)] than the entombing ashfall U-Pb zircon CA-ID-TIMS ages. Our data demonstrate that U-Pb LA-MC-ICP-MS dating of eggshells is remarkably similar in accuracy and precision to LA-ICP-MS U-Pb of detrital zircon from the surrounding sediment and produces MDA ages on par with zircon data. However, via elemental mapping, we have demonstrated that the younger calcite-based age estimate reflects post-depositional mobilization of U and Pb via meteoric waters that permeated the pores, fractures, and fissures of the fossilized eggshell (Fig. 3). Our observations suggest that ootaxa with more porous original ultra- or microstructure, or fossilized eggshell with more diagenetic fracturing (poorer preservation) due to either depositional or post-depositional conditions and/or weaker original ultra- or microstructure, may yield less accurate MDAs; however, broad studies will be needed to study the relationship of these factors to MDA accuracy. In the meantime, our assessment of diagenetic alteration and primary pore structure, and its preliminary relationship with MDA accuracy, highlights the need for more robust diagenetic screening and inter-method cross-validation to assess the reliability of U-Pb ages derived from biogenic carbonates.

Based on the successful application of U-Pb dating to dinosaur eggshells, we tested competing age interpretations for sedimentary strata at the Teel Ulaan Chaltsai locality, yielding excellent results. Of the 381 spots used, only four were discarded, with the resulting spots plotting near-perfectly on the Concordia line of the Tera Wasserburg diagram, indicating closed system behavior of the U-Pb systematics. Our confidence in these age estimates is bolstered by (1) a lack of alteration to the well-preserved eggshell calcite growth textures (biocalcite); (2) an upper intercept Pb-Pb ratio consistent with natural evolution Pb (ca. 0.84) for this period (~75 Ma), indicating no disturbance in the Pb system; and (3) age coherence (within 2%) of each of the four localities across a similar stratigraphic nesting horizon (± 3.5 km laterally). Therefore, the combined age of 75.35 ± 0.74 / 1.5 Ma for all spot analyses from the Teel Ulaan Chaltsai nesting sites is considered a close approximation of the depositional age. In addition to the above results, elemental mapping of the eggshell from Teel Ulaan Chaltsai markedly contrasts with those scanned from the Mussentuchit Member. Rather than a clear post-depositional signature of alteration, elemental mapping demonstrated that absorption of U most likely occurred via meteoric transference at or near the time of initial burial. Minor fluid infiltration during early diagenesis, via meteoric waters and surficial processes, most likely occurred before fossilization. This is supported by our sedimentological work in the area, in agreement with historical observations 35-37, which indicates that fossil assemblages of Teel Ulaan Chaltsai were entombed within pedogenetically altered floodplain fines emplaced by localized crevasse splays and expansive sheet floods. Therefore, we interpret the resulting age as roughly synchronous with the depositional age, but highlight that it should be treated as a maximum depositional age. In such environments, uranium occurs mainly as U(VI), present as soluble uranyl-carbonate complexes (e.g., UO₂(CO₃)₂²⁻, UO₂(CO₃)₃⁴⁻), which readily substitute for Ca²⁺ in the calcite lattice during crystallization, particularly in dense, micritic, low-Mg domains. This process is analogous to U incorporation observed in speleothems and calcretes, where U-Pb dating has proven reliable⁴⁴. Synchrotron-based EXAFS studies show that uranyl ions are accommodated into the calcite structure with varying degrees of distortion depending on time and mineral diagenesis⁴⁵⁻⁴⁷. The homogeneous U distribution observed in LA-ICP-MS elemental mapping (Fig. 3), along with the absence of zoning, redox-sensitive element enrichment (e.g., Mn, Fe), and cathodoluminescence alteration, collectively support early U(VI) uptake during early sediment interation, followed by long-term closed-system behavior. This indicates that the dated calcite preserves its original geochemical signature, validating the reliability of the U-Pb geochronology approach. Alternatively, it is possible, based on the uniform distribution of U and Pb throughout the interior portion of the eggshell, that the U signature reflects the endogenous chemistry of the eggshell during in vivo mineralization as opposed to early meteoric transfer. However, stark differences in U concentration within the eggshell ultrstructure itself (Fig. 3) suggest that this is a highly unlikely scenario. Other than the Bayanshiree Formation (lower post-rift), this is the first time the uppermost post-rift sequences in the Eastern Gobi Basin have been radiometrically calibrated. Our results support the recent hypothesis that these beds are coeval with the Upper Cretaceous Baruungoyot Formation (Fig. 2b)^{36,48}.

The success of U-Pb dating on dinosaur eggshells is accompanied by critical methodological caveats, as observed in studies of modern ostrich eggshells^{25–27}. Firstly, a rigorous pre-screening session via thin-section petrology and eggshell histology to document any potential evidence of diagenesis (e.g., recrystallization). Secondly, this study highlights the prerequisite for meticulous geochemical screening and elemental mapping to identify: (1) reliable U concentrations; (2) evidence of diagenetic alteration; and (3) to avoid areas with common Pb. Additional trace element signatures (REE patterns, Ce anomalies, and Sr-Mn ratios) should be assessed to identify potential diagenetic overprinting¹⁷. Cross-validation with lithostratigraphic and biostratigraphic constraints and independent dating methods is recommended to ensure that the ages reflect the actual time of eggshell deposition rather than subsequent episodes of Pb-loss or resetting due to diagenesis. Lastly, we suggest that future studies collect a suite of samples

(eggshells or nested eggs) across the same stratigraphic horizon to diagnose diagenetic alteration or analytical uncertainties. Beyond methodological considerations, a more significant challenge will be to resolve when the initial uptake of the detectable uranium in the eggshell is introduced: 1) during initial soil contact of the egg(s) in the nest (including partial burial in some taxa) (soil moderated U); or 2) after complete burial (entombment into the sedimentological record) (Fig. 4)^{18,19,49–52}. Despite these challenges, this study demonstrates that eggshell biocalcite from non-avian dinosaurs, birds, and other egg-laying vertebrates has the potential to serve as a reliable geochronometer in Mesozoic and Cenozoic terrestrial sedimentary basins. Continuing investigations into U-uptake and diagenesis of eggshells, methodological advancements will undoubtedly fill key knowledge gaps, resulting in greater accuracy and precision in applying biocalcite as a meaningful tool for age calibration. With further testing and crossvalidation fossilized eggshells represent a potentially significant geochronometer for dating critical fossil deposits in globally dispersed basins lacking datable volcanics (e.g., the Gobi Basin, Mongolia 35-37,48,53,54, or Auca Mahuevo in Patagonia³³, or the Elliot Formation of South Africa⁵⁵).

Methods

The data were acquired using a Thermo Neptune multi-collector inductively coupled plasma mass spectrometer (MC-ICP-MS) coupled to a Photon Machines 193 nm laser ablation system at the Universidade Federal de Ouro Preto. A previous analytical method was adapted 38,56,57. Samples were ablated in a helium atmosphere (0.15 L min⁻¹) and mixed in the ablation funnel with 0.87 L min⁻¹ of argon and 0.02 L min⁻¹ of nitrogen. The ICP-MS was tuned for maximum sensitivity while maintaining oxide formation below 0.2% and preventing fractionation of the Th/U ratio. The laser ablation parameters included static spot sizes of 110 µm, a repetition rate of 5 Hz, a fluence of 6 J cm⁻², a 15-second washout period between analyses, and a 30-second ablation time. For the National Institute of Standards and Technology Standard Reference Material 614 (NIST SRM-614), these settings resulted in a penetration depth of <10 µm and an average sensitivity of 0.005 V for ²³⁸U and 200,000 cps for ²⁰⁶Pb. The detection limits for ²⁰⁶Pb and ²³⁸U were <0.02 ppb and 0.03 ppb, respectively. U-Pb and Pb/ Pb ratios were normalized^{39,40,58}. U-Pb ratios were calibrated using the 254 Ma WC-1 calcite reference material³⁹ and NIST SRM-614. The mean ²⁰⁷Pb/²⁰⁶Pb ratio from each analysis was corrected for mass bias (0.15%), while the 206Pb/238U ratio was corrected for interelement fractionation (~5%), accounting for drift over the sequence duration. Due to the carbonate matrix effects, an additional offset factor of 1.07, determined using WC-1 carbonate reference material³⁹, was applied as an external correction to all carbonate analyses. Data acquisition was performed in fully automated mode overnight. Each study consisted of 20 s of background measurement, 20 s of sample ablation, and a 25-s washout. During the 40-s data collection window, the signals of ²⁰²Hg, ²⁰⁴Pb, ²⁰⁶Pb, and ²⁰⁷Pb were recorded using ion counters, while ²³²Th and ²³⁸U were measured with Faraday cups³⁸.

Time-resolved data reduction was performed using the SATURN software, 6 and all results are presented with a 2σ confidence interval. Multiple analyses were performed on different calcite and dolomite phases, and the data were regressed on Tera-Wasserburg plots using Isoplot (see Supplementary Data and Figshare). Uranium concentrations in samples were estimated by normalizing the signal against WC-1, assuming a U content of approximately 5 ppm. Reported age uncertainties incorporate all analytical errors, as well as the uncertainty associated with the external standard used for normalization. The number of analytical spots used for age calculations relative to the total spots analyzed per phase is presented in Supplementary Data 1 and 2.

Data availability

Data (in-full) from both U-Pb calcite age dating and U-Pb zircon age dating can be found at Figshare: R.T., Venter, K.E., Lana, C., Roberts, E.M., Tsogtbaatar, C., Khishigjav, T., Zanno, L.E., U-Pb calcite age dating of fossil eggshell as an accurate deep time geochronometer. Nature Communications Earth and Environment (2025). Figshare. Dataset.

https://figshare.com/s/3c9faf0f59a5ba51e131. All other information can be requested to the corresponding author (R.T.T.) or the Institute of Paleontology, Mongolian Academy of Sciences (IP-MAS), Ulaanbaatar, Mongolia.

Received: 15 April 2025; Accepted: 8 October 2025; Published online: 10 November 2025

References

- Husson, J. M. & Peters, S. E. Nature of the sedimentary rock record and its implications for Earth system evolution. *Emerg. Top. Life Sci.* 2, 125–136 (2018).
- Gibbard, P. L. & Hughes, P. D. Terrestrial stratigraphical division in the Quaternary and its correlation. *J. Geo. Soc.*, 178, jgs2020–jgs2134 (2021).
- Irmis, R. B., Mundil, R., Martz, J. W. & Parker, W. G. High-resolution U-Pb ages from the Upper Triassic Chinle Formation (New Mexico, USA) support a diachronous rise of dinosaurs. *Earth Plan. Sci. Lett.* 309, 258–267 (2011).
- Langer, M. C., Ramezani, J. & Da Rosa, ÁA. U-Pb age constraints on dinosaur rise from south Brazil. Gond. Res. 57, 133–140 (2018).
- Ramezani, J., Beveridge, T. L., Rogers, R. R., Eberth, D. A. & Roberts, E. M. Calibrating the zenith of dinosaur diversity in the Campanian of the Western Interior Basin by CA-ID-TIMS U-Pb geochronology. Sci. Rep. 12, 16026 (2022).
- Roberts, E. M. et al. New age constraints support a K/Pg boundary interval on Vega Island, Antarctica: Implications for latest Cretaceous vertebrates and paleoenvironments. GSA Bull. 135, 867–885 (2023).
- Tucker, R. T. et al. Exceptional age constraint on a fossiliferous sedimentary succession preceding the Cretaceous Thermal Maximum. Geology 51, 962–967 (2023).
- Wang, T. et al. High-resolution geochronology of sedimentary strata by U-Pb CA-ID-TIMS zircon geochronology: a review. *Earth-Science Rev.* 245, 104550 (2023).
- Eberth, D. A. Stratigraphic architecture of the Belly River Group (Campanian, Cretaceous) in the plains of southern Alberta: Revisions and updates to an existing model and implications for correlating dinosaur-rich strata. PLoS ONE 19, e0292318 (2024).
- Rogers, R. R. et al. Updating the Upper Cretaceous (Campanian) two medicine formation of montana: lithostratigraphic revisions, new CA-ID-TIMS U-Pb ages, and a calibrated framework for dinosaur occurrences. GSA Bull. 137, 315–340 (2025).
- Rossignol, C. et al. Using volcaniclastic rocks to constrain sedimentation ages: To what extent are volcanism and sedimentation synchronous? Sed. Geo. 381, 46–64 (2019).
- Fassett, J. E., Heaman, L. M. & Simonetti, A. Direct U-Pb dating of Cretaceous and paleocene dinosaur bones, San Juan Basin, New Mexico. *Geology* 39, 159–162 (2011).
- 13. Qi, L. et al. In situ U-Pb dating of Jurassic dinosaur bones from Sichuan Basin, South China. *Geology* **52**, 216–221 (2024).
- Rochín-Bañaga, H. & Davis, D. W. Insights into U-Th-Pb mobility during diagenesis from laser ablation U-Pb dating of apatite fossils. Chem. Geo. 618, 121290 (2023).
- Gruen, R. & Stringer, C. Direct dating of human fossils and the everchanging story of human evolution. *Quat. Sci. Rev.* 322, 108379 (2023).
- 16. Dirks, P. H. et al. The age of Homo Naledi and associated sediments in the Rising Star Cave, South Africa. *Elife* **6**, e24231 (2017).
- Tanabe, M. et al. Apatite U-Pb dating of dinosaur teeth from the Upper Cretaceous Nemegt Formation in the Gobi Desert, Mongolia: Contribution to depositional age constraints. *Island Arc* 32, e12488 (2023).
- Graf, J. et al. Diagenesis of dinosaur eggshell from the Gobi Desert, Mongolia. Palaeogeogr. Palaeoclimatol. Palaeoecol. 494, 65–74 (2018).
- Fanti, F. et al. Geochemical fingerprinting as a tool for repatriating poached dinosaur fossils in Mongolia: a case study for the Nemegt

- Locality, Gobi Desert. *Palaeogeogr. Palaeoclimatol. Palaeoecol.* **494**, 51–56 (2018).
- Keenan, S. W. From bone to fossil: a review of the diagenesis of bioapatite. Am. Miner. 101, 1943–1951 (2016).
- Senter, P. J. Radiocarbon in dinosaur fossils: compatibility with an age of millions of years. Am. Bio. Tea. 82, 72–79 (2020).
- Senter, P. J. Radiocarbon in dinosaur bones revisited: Problems with collagen. Am. Bio. Tea. 84, 336–341 (2022).
- Roberts, N. M. et al. LA-ICP-MS U-Pb carbonate geochronology: strategies, progress, and application to fracture-fill calcite. *Geoch. Disc.* (2020).
- Woodhead, J. & Petrus, J. Exploring the advantages and limitations of in situ U–Pb carbonate geochronology using speleothems. *Geochron* 1, 69–84 (2019).
- Miller, J. M. & Willoughby, P. R. Radiometrically dated ostrich eggshell beads from the Middle and Later Stone Age of Magubike Rockshelter, southern Tanzania. J. Hum. Evol. 74, 118–122 (2014).
- Janz, L., Feathers, J. K. & Burr, G. S. Dating surface assemblages using pottery and eggshell: assessing radiocarbon and luminescence techniques in Northeast Asia. J. Arch. Sci. 57, 119–129 (2015).
- Sharp, W. D. et al. 230Th/U burial dating of ostrich eggshell. *Quat. Sci. Rev.* 219, 263–276 (2019).
- Andrews, R. C. Explorations in Mongolia: a review of the Central Asiatic expeditions of the American Museum of Natural History. Geo. J. 69, 1–19 (1927).
- 29. Zhao, Z. Progress in the research of dinosaur eggs. Mesoz Cenozoic Red Beds South China, 330–340 (1979).
- Dong, Z. M. & Currie, P. J. Protoceratopsian embryos from Inner Mongolia, People's Republic of China. Can. J. E. Sci. 30, 2248–2254 (1993).
- He, Q. et al. Isotope compositions of dinosaur eggs and associated depositional settings in the Upper Cretaceous Huizhou Formation from the Qiyunshan area, Anhui Province, China: implications for paleoenvironmental reconstruction. *Hist. Biol.* 35, 1197–1208 (2023).
- Wu, R. et al. The smallest known complete dinosaur fossil eggs from the Upper Cretaceous of South China. *Hist. Biol.* 1–10 https://doi.org/ 10.1080/08912963.2024.2409873 (2024).
- Chiappe, L. M. et al. Sauropod dinosaur embryos from the Late Cretaceous of Patagonia. *Nature* 396, 258–261 (1998).
- Lawver, D. R., Rasoamiaramanana, A. H. & Werneburg, I. An occurrence of fossil eggs from the Mesozoic of Madagascar and a detailed observation of eggshell microstructure. *J. Vert. Paleo.* 35, e973030 (2015).
- Watabe, M., Tsogtbaatar, K., Suzuki, S. & Saneyoshi, M. Geology of dinosaur-fossil-bearing localities (Jurassic and Cretaceous: Mesozoic) in the Gobi Desert: results of the HMNS-MPC joint paleontological expedition. *Hayashibara Mus. Nat. Sci. Res. Bull.* 3, 41–118 (2010).
- Mikhailov, K. E. Classification of fossil eggshells of amniotic vertebrates. Acta Palaeo. Pol. 36 (1991).
- Balzhinyam, L. 1: 200,000 Scale Geological Map of Mongolia; 1st edn. L-49-XXVII Sainshand (eds Timurtogo, O., Minjin, Ch., Gera, O., and Dorjnamjaa) (Ministry of Industry and Commerce, Petroleum Geological Information Center, 2007).
- Lana, C. et al. Characterization of zircon reference materials via high precision U-Pb LA-MC-ICP-MS. J. Anal. At. Spectrom. 32, 2011–2023 (2017).
- Roberts, N. et al. A calcite reference material for LA-ICP-MS U-Pb geochronology. Geochem. Geophys. Geosyst. 18, 2807–2814 (2017).
- Roberts, N. M. et al. Laser ablation inductively coupled plasma mass spectrometry (LA-ICP-MS) U-Pb carbonate geochronology: strategies, progress, and limitations. *Geochron* 2, 33–61 (2020).
- Tucker, R. T., Zanno, L. E., Huang, H. Q. & Makovicky, P. J. A refined temporal framework for newly discovered fossil assemblages of the upper Cedar Mountain Formation (Mussentuchit Member), Mussentuchit Wash, Central Utah. Cret. Res. 110 (2020).

- Tucker, R. T., Suarez, C. A., Makovicky, P. J. & Zanno, L. E. Paralic sedimentology of the Mussentuchit Member coastal plain, Cedar Mountain Formation, central Utah, USA. J. Sed. Res. 92, 546–569 (2022).
- Hedge J., Tucker R. T., Makovicky P. J. & Zanno L. E. Fossil Eggshell Diversity of the Mussentuchit Member, Cedar Mountain Formation, Utah. PLoS ONE 20, e0314689 (2025).
- Rasbury, E. T. & Cole, J. M. Directly dating geologic events: U-Pb dating of carbonates. R. Geoph. 47 (2009).
- 45. Kelly, S. D. et al. Uranyl incorporation in natural calcite. *Environ. Sci. Technol.* **37**, 1284–1287 (2003).
- Kelly, S. D., Rasbury, E. T., Chattopadhyay, S., Kropf, A. J. & Kemner, K. M. Evidence of a stable uranyl site in ancient organic-rich calcite. *Environ. Sci. Technol.* 40, 2262–2268 (2006).
- Sturchio, N. C., Antonio, M. R., Soderholm, L., Sutton, S. R. & Brannon, J. C. Tetravalent uranium in calcite. *Science* 281, 971–973 (1998).
- Eberth, D. A. Stratigraphy and paleoenvironmental evolution of the dinosaur-rich Baruungoyot-Nemegt succession (Upper Cretaceous), Nemegt Basin, southern Mongolia. *Palaeogeogr. Palaeoclimatol. Palaeoecol.* 494, 29–50 (2018).
- Leuzinger, L. et al. Life and reproduction of titanosaurians: Isotopic hallmark of mid-palaeolatitude eggshells and its significance for body temperature, diet, and nesting. *Chem. Geol.* 583, 120452 (2021).
- Niespolo, E. M. et al. December. Patterns of U uptake and implications for diagenesis and trace element records in biomineral eggshell. In AGU Fall Meeting Abstracts 2019, PP34 2019).
- 51. Kim, N., Niespolo, E. M. & Varricchio, D. Testing Dinosaur Eggshells for U-Pb Dating. *AGU24* (2024).
- Niespolo, E., Kim, N., Kracht, O. & Akhtar, A. Trace element profiling in Cenozoic avian eggshells and implications for U-daughter dating. AGU24 (2024).
- Eberth, D. A. et al. Assignment of Yamaceratops dorngobiensis and associated redbeds at Shine Us Khudag (Eastern Gobi, Dorngobi Province, Mongolia) to the redescribed Javkhlant Formation (Upper Cretaceous). J. Vert. Paleo. 29, 295–302 (2009).
- 54. Jerzykiewicz, T., Currie, P. J., Fanti, F. & Lefeld, J. Lithobiotopes of the Nemeqt Gobi Basin1. *Can. J. E. Sci.* **58**, 829–851 (2021).
- Zelenitsky, D. K. & Modesto, S. P. Re-evaluation of the eggshell structure of eggs containing dinosaur embryos from the Lower Jurassic of South Africa. S. Afr. J. Sci. 98, 407–408 (2002).
- Caxito, F. et al. Goldilocks at the dawn of complex life: mountains might have damaged Ediacaran–Cambrian ecosystems and prompted an early Cambrian greenhouse world. Sci. Rep. 11, 20010 (2021).
- de Carvalho, D. F. et al. Constraining the diagenesis of the Puga cap carbonate from U-Pb in-situ dating of seafloor crystal fans, southern Amazonian craton, Brazil. *Terra Nova* 35, 276–284 (2023).
- Silva, J. P., Lana, C., Mazoz, A., Buick, I. & Scholz, R. U-Pb Saturn: New U-Pb/Pb-Pb Data Reduction Software for LA-ICP-MS. Geostan. Geoan. Res. 47, 49–66 (2023).
- 59. Carpenter, K. Eggs, Nests, and Baby Dinosaurs: A Look at Dinosaur Reproduction (Indiana University Press, 1999).
- Paik, I. S., Lee, Y. I., Kim, H. J. & Huh, M. Time, space and structure on the Korea Cretaceous Dinosaur Coast: Cretaceous stratigraphy, geochronology, and paleoenvironments. *Ichnos* 19, 6–16 (2012).
- Tucker, R. T. et al. Geological and paleontological reconstruction of the Bayanshiree Formation, Eastern Gobi Basin, Mongolia. Sed. (SED--OA-032.) (2025) In Review.
- van Niekerk, J. B. et al. Geological reassessment of syn-rift extensional sequences in the Shine Usny Tolgod and Dzun Shakhai fossil localities, Eastern Gobi Basin, Mongolia. Sed 72, 1275–1315 (2025).
- Roberts, E. M. et al. Revised stratigraphy and age of the Red Sandstone Group in the Rukwa Rift basin, Tanzania. Cret. Res. 25, 749–759 (2004).

- Hicks, J. F., Brinkman, D. L., Nichols, D. J. & Watabe, M.
 Paleomagnetic and palynologic analyses of Albian to Santonian strata at Bayn Shireh, Burkhant, and Khuren Dukh, eastern Gobi Desert, Mongolia. Cret. Res. 20, 829–850 (1999).
- Shuvalov, V. F. in *The Age of Dinosaurs in Russia and Mongolia* (eds. Benton, M. J., Shishkin, M. A., Unwin, D. M. & Kurochkin, E. N.) 256e278 (Cambridge University Press, 2000).
- Van Itterbeeck, J., Horne, D. J., Bultynck, P. & Vandenberghe, N. Stratigraphy and palaeoenvironment of the dinosaur-bearing Upper Cretaceous Iren Dabasu Formation, Inner Mongolia, People's Republic of China. Cret. Res. 26, 699–725 (2005).
- Johnson, C. L. Polyphase evolution of the East Gobi basin: sedimentary and structural records of Mesozoic–Cenozoic intraplate deformation in Mongolia. *Basin Res.* 16, 79–99 (2004).

Acknowledgements

The authors thank the staff, students, and volunteers of the Institute of Paleontology of the Mongolian Academy of Sciences, the North Carolina Museum of Natural Sciences, and the Department of Earth Sciences, Stellenbosch University, who participated in the 2022-2023 MADEx expeditions. S. Moran (NCSM), D. Idersaikhan (IP-MAS), and E. Monkhtor (IP-MAS), for shipping. Sampling and analysis were done in accordance with the BLM (Mussentuchit) and IP-MAS (Teel Ulaan Chaltsai). Financial support was provided by the National Geographic Society (NGS-100601R-23) to L.E.Z, R.T.T, and T.C. and a National Science Foundation (award #1925973 to L.E.Z and R.T.T.).

Author contributions

R.T.T., C.L., and L.E.Z. Conceived the study in collaboration with E.M.R., K.T., and T.C. K.E.V. and R.T.T. oversaw all aspects of the study, including sample collection, and led in writing the paper. C.L. carried out all analytical observations, performed the analysis, conducted data reduction, and presented the final ages along with financial support for the analytical-based portions of this study. L.E.Z. and T.C. aided in field-based collections, egg and eggshell identification and classification, critical comments during manuscript preparations, and provided financial support for field-based portions of this study. T.C. and K.T. provided access and facilitated permits to sites within the Gobi Basin, as well as offered comments during the later stages of manuscript preparation. E.M.R. assisted with writing and conceptual feedback of the manuscript.

Competing interests

The authors declare no competing interests.

Additional information

Supplementary information The online version contains supplementary material available at https://doi.org/10.1038/s43247-025-02895-w.

Correspondence and requests for materials should be addressed to Ryan T. Tucker.

Peer review information Communications Earth and Environment thanks Octávio Mateus, E. Martín Hechenleitner for their contribution to the peer review of this work. Primary Handling Editors: Yuan Shang, Carolina Ortiz Guerrero, and Mengjie Wang. A peer review file is available].

Reprints and permissions information is available at http://www.nature.com/reprints

Publisher's note Springer Nature remains neutral with regard to jurisdictional claims in published maps and institutional affiliations.

Open Access This article is licensed under a Creative Commons Attribution-NonCommercial-NoDerivatives 4.0 International License, which permits any non-commercial use, sharing, distribution and reproduction in any medium or format, as long as you give appropriate credit to the original author(s) and the source, provide a link to the Creative Commons licence, and indicate if you modified the licensed material. You do not have permission under this licence to share adapted material derived from this article or parts of it. The images or other third party material in this article are included in the article's Creative Commons licence, unless indicated otherwise in a credit line to the material. If material is not included in the article's Creative Commons licence and your intended use is not permitted by statutory regulation or exceeds the permitted use, you will need to obtain permission directly from the copyright holder. To view a copy of this licence, visit http://creativecommons.org/licenses/by-nc-nd/4.0/.

© The Author(s) 2025